Exp Brain Res (2003) 151:145–157
DOI 10.1007/s00221-003-1443-3

RESEARCH ARTICLE

David W. Franklin · Etienne Burdet · Rieko Osu · Mitsuo Kawato · Theodore E. Milner

Functional significance of stiffness in adaptation of multijoint arm movements to stable and unstable dynamics

Received: 26 August 2002 / Accepted: 5 February 2003 / Published online: 29 May 2003

Abstract This study compared the mechanisms of adaptation to stable and unstable dynamics from the perspective of changes in joint mechanics. Subjects were instructed to make point to point movements in force fields generated by a robotic manipulandum which interacted with the arm in either a stable or an unstable manner. After subjects adjusted to the initial disturbing effects of the force fields they were able to produce normal straight movements to the target. In the case of the stable interaction, subjects modified the joint torques in order to appropriately compensate for the force field. No change in joint torque or endpoint force was required or observed in the case of the unstable interaction. After adaptation, the endpoint stiffness of the arm was measured by applying displacements to the hand in eight different directions midway through the movements. This was compared to the stiffness measured similarly during movements in a null force field. After adaptation, the endpoint stiffness under both the stable and unstable dynamics was modified relative to the null field. Adaptation to unstable dynamics was achieved by selective modification of endpoint stiffness in the direction of the instability. To investigate whether the change in endpoint stiffness could be accounted for by change in joint torque or endpoint force, we estimated the change in stiffness on each trial based on the change in joint torque relative to the null field. For stable dynamics the change in endpoint stiffness was accurately predicted. However, for unstable dynamics the change in endpoint stiffness could not be reproduced. In fact, the predicted endpoint stiffness was similar to that in the null force field. Thus, the change in endpoint stiffness seen after adaptation to stable dynamics was directly related to changes in net joint torque necessary to compensate for the dynamics in contrast to adaptation to unstable dynamics, where a selective change in endpoint stiffness occurred without any modification of net joint torque.

Keywords Stability · Motor learning · Impedance control · Endpoint stiffness · Inverse dynamics model

D. W. Franklin (✉) · R. Osu · M. Kawato
ATR Computational Neuroscience Laboratories,
2-2-2 Hikaridai, Seika-cho, Soraku-gun, 619-0288 Kyoto, Japan
e-mail: dfrank@atr.co.jp
Tel.: +81-774-951082
Fax: +81-774-952647

D. W. Franklin · T. E. Milner
School of Kinesiology, Simon Fraser University,
Burnaby, B.C., V5A 1S6, Canada

E. Burdet
Department of Mechanical Engineering
and Division of Bioengineering,
National University of Singapore, 119260 Singapore

Introduction

We constantly interact with the world around us, moving and manipulating objects in our environment. Tasks such as opening a door, which involve a stable interaction with the environment, are relatively simple to learn, because similar motor commands will result in similar movements, so the dynamics can be easily identified and compensated. For example, we may be surprised the first time we open a door with high friction, but will be able to open the door smoothly on the second or third trial. Unstable tasks are more difficult to learn, because they are affected by different initial conditions, neuromotor noise (Schmidt et al. 1979; Slifkin and Newell 1999), or any small external perturbation, which can lead to unpredictable, inconsistent, and unsuccessful performance. For example, during sculpting, material irregularities can displace the chisel to the left or to the right of the intended path, and it requires extensive practice for a sculptor to acquire the skill necessary to compensate for such instability.

Many tasks that humans perform, particularly those involving tool use, are inherently unstable (Rancourt and Hogan 2001). However, while the tasks may be unstable, the mechanical impedance of the musculoskeletal system, which is stabilizing in nature, counteracts the instability.

Ultimately, it is the interaction between our limbs and the environment that determines whether or not a movement will be stable. Coupled stability of the limb and the environment is a prerequisite for successful actions, as it provides robustness to motor output variability and perturbations from the environment. Limb impedance can be modified by changing the force at the hand since muscle stiffness inherently scales with activation level (Hunter and Kearney 1982). Modification of impedance geometry, for example, shape and/or orientation of endpoint stiffness, has been reported (Gomi and Osu 1998; Lacquaniti et al. 1993; McIntyre et al. 1996) but is generally associated with a change in applied force, or a change in the limb configuration. Such inherent modulation of impedance with applied force often cannot be used to achieve stability, for example, when the task constrains the direction or magnitude of the hand force. Similarly, task demands may limit the variation in the endpoint impedance that could be achieved by changing the limb configuration. To deal with such situations, the CNS must be able to modify the size, shape, or orientation of the impedance independently of the force applied by the hand. This could be achieved by co-contracting specific groups of muscles to select the geometry of the endpoint stiffness (Hogan 1985). We have recently demonstrated that the CNS can optimize the magnitude, shape, and orientation of the endpoint stiffness of the arm to compensate for environmental instabilities (Burdet et al. 2001).

If the CNS is concerned about minimizing metabolic cost then we would expect that the endpoint stiffness, in tasks which are mechanically stable, would be directly related to the minimum muscle torque necessary to move the arm and compensate for any external dynamics. Specifically, if metabolic energy is to be minimized, then muscles will be recruited with the minimal activation so as to produce the desired net joint torques. Accordingly, we would expect a relatively linear relation between joint torque and joint stiffness similar to that found under stable isometric conditions (Gomi and Osu 1998; Perreault et al. 2001) as muscle and joint stiffness have been found to increase monotonically with muscle force and joint torque, respectively (Gottlieb and Agarwal 1988; Hunter and Kearney 1982; Kirsch et al. 1994; Milner et al. 1995). It should, therefore, be possible to predict the joint stiffness from the net torque generated by muscles during performance of the task. This is in contrast to tasks which require greater stability than would be conferred by the minimum muscle activation necessary to move the arm and compensate for any external dynamics. Under such unstable conditions, co-contraction of opposing muscles may be required above and beyond that ordinarily occurring with the movement. In such cases, the joint stiffness should be higher than that predicted by the net joint torque.

The present study was undertaken to analyze and compare adaptation to environments producing stable or unstable interactions with the arm from the perspective of changes in limb mechanics. Previously, we measured the endpoint stiffness of the arm after adaptation to mechanical instability and found a selective increase in stiffness in the direction of instability, which appeared to compensate precisely for the instability (Burdet et al. 2001). We extend that work in the current paper by presenting new data and analysis of stiffness after adaptation to instability, as well as examining stiffness after adaptation to stable dynamics. Adaptation to stable dynamics, which has been examined previously by looking at kinematics and EMG (Shadmehr and Mussa-Ivaldi 1994; Thoroughman and Shadmehr 1999), has never been characterized in terms of the change in endpoint stiffness. In order to properly compare and contrast the adaptation to stable and unstable environments we rigorously modeled the trial to trial variation in the force response to displacement. We investigated whether the change in stiffness observed after adaptation to the stable or unstable environment was controlled independently of the change in joint torque needed to compensate for the new dynamics. In an unstable environment, the change in stiffness was independent of the change in joint torque. However, in a stable environment, we found that changes in endpoint stiffness were well correlated with changes in joint torque. Therefore, while the change in endpoint stiffness in the unstable environment was directly controlled and could be attributed to adaptive co-contraction of antagonist muscle pairs, the change in endpoint stiffness in the stable force field reflected only the adaptive change in joint torque.

Materials and methods

Six healthy individuals participated in the study (20–34 years of age; two females and four males). The institutional ethics committee approved the experiments and the subjects gave informed consent prior to participation.

Apparatus

Subjects sat in a chair and moved the parallel-link direct drive air-magnet floating manipulandum (PFM) in a series of forward reaching movements performed in the horizontal plane. Their shoulders were held against the back of the chair by means of a shoulder harness. The right forearm was securely coupled to the PFM using a rigid custom molded thermoplastic cuff. The cuff immobilized the wrist joint, permitting movement of only the shoulder and elbow joints. The subjects' right forearm rested on a support beam projecting from the handle of the PFM. Motion was, therefore, limited to a single degree of freedom at the shoulder and at the elbow. The manipulandum and setup are described in detail elsewhere (Gomi and Kawato 1996, 1997). In brief, the subjects' hand position was measured with joint-position sensors (409 600 pulse/rev) and the force exerted by the hand was measured using a force sensor located between the handle and the manipulandum (resolution 0.059 N). Position and force were sampled at 500 Hz.

Subjects performed reaching movements from a start circle located 0.31 m in front of the shoulder to a target circle located 0.56 m in front of the shoulder (total distance 0.25 m). The start and target circles along with the instantaneous hand position were projected down onto an opaque horizontal surface located directly overtop of the subjects arm. This surface also removed the subject's arm from view.

Force fields

The experiment examined stiffness and EMG adaptation in two force fields: a velocity-dependent force field (VF), producing a stable interaction with the arm, and a position-dependent (divergent) force field (DF), producing an unstable interaction. Results were compared to those in a null field (NF). The force (F_x, F_y) (in N) exerted on the hand by the robotic interface in the VF was computed as:

$$\begin{bmatrix} F_x \\ F_y \end{bmatrix} = \chi \begin{bmatrix} 13 & -18 \\ 18 & 13 \end{bmatrix} \begin{bmatrix} \dot{x} \\ \dot{y} \end{bmatrix} \quad (1)$$

where ($\dot{x}$, $\dot{y}$) is the hand velocity (m/s) and the scaling factor, χ, was adjusted to the subject's strength ($2/3 \leq \chi \leq 1$). In particular, χ was 2/3 for women, 15/18 for most men, and 1 for the largest men. The DF produced a negative elastic force perpendicular to the target direction with a value of zero along the *y*-axis, i.e., no force was exerted when trajectories followed the *y*-axis, but the hand was pushed away whenever it deviated from the *y*-axis. The DF was implemented as:

$$\begin{bmatrix} F_x \\ F_y \end{bmatrix} = \begin{bmatrix} \beta x \\ 0 \end{bmatrix} \quad (2)$$

where the *x*-component of the hand position was measured relative to the shoulder joint. $\beta > 0$ (N/m) was adjusted for each subject so that it was larger than the stiffness of the arm measured in NF movements so as to produce an unstable interaction. Both force fields were inactivated once the subject reached the target position.

Learning

All subjects practiced making movements in the NF on at least 1 day prior to the experiment. These training trials were used to accustom the subjects to the equipment and to the movement speed and accuracy requirements. Subjects were randomly assigned to one of two groups. Group 1 initially performed the experiments with the DF, and then proceeded to the VF, whereas group 2 adapted to the fields in reverse order. Stiffness was normally measured the day after adaptation to a particular force field once sufficient practice in the field had taken place (see impedance estimation below).

Subjects first practiced in the NF until they had achieved 50 successful trials. Successful trials were those which ended inside the 2.5-cm-diameter target window within the prescribed time (0.6±0.1 s). All movements were recorded whether successful or not. Movements were self-paced so subjects were able to rest between movements if they wished. At the completion of 50 successful trials, the force field was activated. No information was given to the subjects as to when the force field trials would begin. Subjects then practiced in the force field until achieving 75 successful trials. They took a short break and then performed 100 more movements, 20 of which were random trials in the NF. The NF trials were called after-effects and were recorded to confirm that subjects adapted to the force field.

Impedance estimation

We measured stiffness in VF and DF movements after extensive learning, as well as in NF movements. The method is described in detail by Burdet et al. (2000). Prior to each stiffness measurement session, the subjects were retrained in the force field to ensure that they had readapted to the field (NF: 40 trials; DF, VF: 80 trials). For three subjects, 160 movements were then performed in each force field, of which 80 were randomly selected for stiffness measurement. For one subject, in the case of all three force fields, and for two other subjects, in the case of two of the force fields, only 80 movements were performed. Half of these were randomly selected for stiffness measurement (as in Burdet et al. 2001). On these trials, displacements were introduced at the midpoint of the movement in one of eight directions chosen randomly from the set {0°, 45°, 90°, 135°, 180°, 225°, 270°, 315°}. The PFM briefly displaced the hand by a constant distance from a prediction of the undisturbed trajectory (Burdet et al. 2000). This displacement had an amplitude of 8 mm and lasted 300 ms. This was composed of a 100-ms ramp away from the current trajectory, a 100-ms hold portion, and a 100-ms ramp back toward the predicted trajectory. During the hold phase of the perturbation, the hand was displaced with the predicted velocity of the unperturbed movement. Assuming that the prediction is perfect there would be no difference in velocity between the perturbed and unperturbed trajectories, eliminating any contribution of damping to the change in measured endpoint force. Although the prediction is not perfect, our results indicate that the errors are small and that the average prediction over several trials is very close to the average of the actual trajectory (Burdet et al. 2000). Therefore, we can be quite confident that forces due to damping did not introduce error in the stiffness measurements. Using the average force and displacement during a 60-ms interval toward the end of the hold portion of the perturbation window, an estimate of the 2×2 endpoint stiffness matrix (**K**) was obtained by linear regression of the mean change in hand force and the mean change in position, as represented by the equation:

$$\begin{bmatrix} \Delta F_x \\ \Delta F_y \end{bmatrix} = \mathbf{K} \begin{bmatrix} \Delta x \\ \Delta y \end{bmatrix} \quad (3)$$

The stiffness in different directions was represented in terms of an ellipse by plotting the elastic force produced by a unit displacement (Mussa-Ivaldi et al. 1985).

In the perturbation trials in the VF, the force field was activated prior to and after the perturbation to ensure that the same trajectory and motor commands were used in the perturbation and non-perturbation trials. In the trials where the hand was displaced in the DF, the force field was not activated prior to the displacement in order to avoid amplification of trajectory deviations that would contribute to error in the stiffness estimates. Since subjects could not detect the absence of the force field on these trials we were able to rule out the possibility that changes in stiffness were reactive to the environment.

The joint stiffness (**R**) was calculated from the endpoint stiffness (**K**) using the relation:

$$\mathbf{R} = \begin{bmatrix} \mathrm{R}_{ss} & \mathrm{R}_{se} \\ \mathrm{R}_{es} & \mathrm{R}_{ee} \end{bmatrix} = \mathbf{J}^T \mathbf{K} \mathbf{J} + \frac{\partial \mathbf{J}^T}{\partial \theta} \mathbf{F} \quad (4)$$

where **J** is the Jacobian, a matrix which represents the geometric transformation of small changes in joint angles to small changes in endpoint position, and **F** is the endpoint force (McIntyre et al. 1996).

Stiffness dependence on joint torque

Previously, it had been shown that joint stiffness linearly increases with joint torque during postural tasks (Gomi and Osu 1998). Recently however, we demonstrated that the endpoint stiffness after adaptation to an unstable force field (DF) was selectively increased along the *x*-axis without any corresponding mean change in net joint torque (Burdet et al. 2001). However, even if the mean change in joint torque is zero, this does not mean that the stiffness could not be produced by variations in the joint torque from trial to trial which sum to zero over the entire experiment. Previously, we looked for a simple correlation between the actual endpoint force in the *x*-direction and the expected force based on the measured stiffness and the size of the displacement. A more rigorous approach has been taken in the current work, which considers the forces and stiffness in both the *x*- and *y*-directions. We wish to examine whether trial to trial variation in net muscle torque is correlated with the variation in measured stiffness. In the previous approach we calculated muscle torque from the endpoint force recorded during the perturbation. This value includes not only the force which would be produced by muscles during a normal

movement but also the elastic force resisting the perturbation. Consequently, part of the measured force would have been correlated a priori with the expected change in force calculated from the measured stiffness. To avoid this confounding effect we have estimated the force necessary to compensate for the force field using our trajectory prediction algorithm (Burdet et al. 2000). For each trial, we use the trajectory in the first portion of the movement along with information from previous trials to predict what the trajectory would have been without the perturbation. From this trajectory we could determine the force that the force field would have applied to the subject to obtain a more accurate estimate of the net muscle torque at each joint. In this way, it is possible to investigate whether or not the changes in stiffness in the VF and DF are dependent or independent of any change in joint torque while avoiding the confounding effects of the perturbations.

The following formulas use three different symbols to denote differences in variables: d, δ, and Δ. For example, when referring to torque, d refers to the change in joint torque, $d\tau$, produced by displacing the hand, i.e., the torque resisting the displacement, δ refers to the difference between the resisting torque, $d\tau$, in one force field and $d\tau$ in a different force field, and Δ refers to the difference between the joint torque required to move the arm in one force field and the joint torque required for the same movement in a different force field.

When the arm is constrained to move in the horizontal plane at shoulder height, as in this experiment, it can be modeled as a two degree-of-freedom mechanical system. The associated 2×2 joint stiffness matrix $\mathbf{R}$ is defined by:

$$\begin{bmatrix} d\tau_s \\ d\tau_e \end{bmatrix} = \begin{bmatrix} R_{ss} & R_{se} \\ R_{es} & R_{ee} \end{bmatrix} \begin{bmatrix} d\theta_s \\ d\theta_e \end{bmatrix} \tag{5}$$

where the change in joint torque $d\tau=[d\tau_s\ d\tau_e]^{\mathrm{T}}$ is the elastic resistance to a differential displacement $d\theta=[d\theta_s\ d\theta_e]^{\mathrm{T}}$. The stiffness $\mathbf{R}$ can be estimated during arm movements by measuring the restoring force in response to small perturbations relative to a prediction of the undisturbed trajectory (Burdet et al. 2000). As we wish to examine the change in stiffness that occurs during the adaptation to the force fields, the change in torque associated with joint stiffness in the NF

$$\begin{bmatrix} d\tau_s^{NF} \\ d\tau_e^{NF} \end{bmatrix} = \begin{bmatrix} R_{ss}^{NF} & R_{se}^{NF} \\ R_{es}^{NF} & R_{ee}^{NF} \end{bmatrix} \begin{bmatrix} d\theta_s \\ d\theta_e \end{bmatrix}$$

is subtracted from the change in torque associated with joint stiffness in the force field

$$\begin{bmatrix} d\tau_s^{FF} \\ d\tau_e^{FF} \end{bmatrix} = \begin{bmatrix} R_{ss}^{FF} & R_{se}^{FF} \\ R_{es}^{FF} & R_{ee}^{FF} \end{bmatrix} \begin{bmatrix} d\theta_s \\ d\theta_e \end{bmatrix}$$

resulting in

$$\begin{bmatrix} \delta\tau_s \\ \delta\tau_e \end{bmatrix} = \begin{bmatrix} \Delta R_{ss} & \Delta R_{se} \\ \Delta R_{es} & \Delta R_{ee} \end{bmatrix} \begin{bmatrix} d\theta_s \\ d\theta_e \end{bmatrix} \tag{6}$$

where,

$$\begin{bmatrix} \Delta R_{ss} & \Delta R_{se} \\ \Delta R_{es} & \Delta R_{ee} \end{bmatrix} = \begin{bmatrix} R_{ss}^{FF} - R_{ss}^{NF} & R_{se}^{FF} - R_{se}^{NF} \\ R_{es}^{FF} - R_{es}^{NF} & R_{ee}^{FF} - R_{ee}^{NF} \end{bmatrix}$$

$$\begin{bmatrix} \delta\tau_s \\ \delta\tau_e \end{bmatrix} = \begin{bmatrix} d\tau_s^{FF} - d\tau_s^{NF} \\ d\tau_e^{FF} - d\tau_e^{NF} \end{bmatrix}$$

and the change in joint angle $d\theta$ is assumed to be the same in all force fields.

Joint stiffness has been shown to be well correlated with joint torque for single joints such as the ankle (Hunter and Kearney 1982), elbow (Cannon and Zahalak 1982), wrist (Milner et al. 1995), and interphalangeal joints of the thumb (Akazawa et al. 1983) and index finger (Carter et al. 1990) during maintenance of posture, and for the elbow during movement (Bennett 1993). Similar correlations between joint stiffness and joint torque have been found during maintenance of multijoint posture of the arm (Gomi and Osu 1998; McIntyre et al. 1996). Gomi and Osu (1998) showed that: (1) the shoulder stiffness R_{ss} was well correlated with shoulder torque $|\tau_s|$ and weakly correlated with the elbow torque $|\tau_e|$, (2) the cross-joint stiffness elements R_{se} and R_{es} are of similar magnitude, well correlated with $|\tau_e|$ but poorly correlated with $|\tau_s|$, and (3) the elbow stiffness is well correlated with $|\tau_e|$ and weakly with $|\tau_s|$. However, as the biarticular muscles should contribute to all four elements of the joint stiffness matrix, and as biarticular muscle activation may be much higher during movement as compared to isometric tasks (van Groeningen and Erkelens 1994; Karst and Hasan 1991; Tax et al. 1989, 1990a, b), the shoulder stiffness term may vary as a function of both $|\tau_s|$ and $|\tau_e|$. The presence of the elbow torque term in the expression for shoulder stiffness reflects the contribution of the biarticular muscles which have been shown to be activated primarily to produce elbow torque (Buchanan et al. 1986; Flanders and Soechting 1990; Gomi and Osu 1998; Osu and Gomi 1999; Wadman et al. 1980). In particular, we assumed that the dependence of joint stiffness on joint torque could be represented as:

$$\mathbf{R}^{NF} = \begin{bmatrix} \alpha_1\left|\tau_s^{NF}\right| + \alpha_2\left|\tau_e^{NF}\right| & \alpha_3\left|\tau_e^{NF}\right| \\ \alpha_3\left|\tau_e^{NF}\right| & \alpha_4\left|\tau_e^{NF}\right| \end{bmatrix} + \mathbf{R}_{\mathrm{p}}, \alpha_1 \ldots \alpha_4 \text{constants} \tag{7}$$

and

$$\mathbf{R}^{FF} = \begin{bmatrix} \alpha_1\left|\tau_s^{FF}\right| + \alpha_2\left|\tau_e^{FF}\right| & \alpha_3\left|\tau_e^{FF}\right| \\ \alpha_3\left|\tau_e^{FF}\right| & \alpha_4\left|\tau_e^{FF}\right| \end{bmatrix} + \mathbf{R}_{\mathrm{p}}, \alpha_1 \ldots \alpha_4 \text{constants} \tag{8}$$

where $\mathbf{R}_{\mathrm{p}}$ is the passive stiffness. Subtracting Eq. 7 from Eq. 8 yields:

$$\Delta\mathbf{R} = \begin{bmatrix} \alpha_1\Delta|\tau_s| + \alpha_2\Delta|\tau_e| & \alpha_3\Delta|\tau_e| \\ \alpha_3\Delta|\tau_e| & \alpha_4\Delta|\tau_e| \end{bmatrix}, \alpha_1 \ldots \alpha_4 \text{constants} \tag{9}$$

where

$$\begin{bmatrix} \Delta|\tau_s| \\ \Delta|\tau_e| \end{bmatrix} = \begin{bmatrix} \left|\tau_s^{FF}\right| - \left|\tau_s^{NF}\right| \\ \left|\tau_e^{FF}\right| - \left|\tau_e^{NF}\right| \end{bmatrix}$$

Equation 6 was transformed from joint co-ordinates to endpoint co-ordinates to obtain the relation:

$$\Delta\mathbf{F} = \left(\mathbf{J}^{-1}\right)^T \Delta\mathbf{R} \begin{bmatrix} d\theta_s \\ d\theta_e \end{bmatrix} \tag{10}$$

As the trajectories of movements in the VF and DF after learning were similar to movements in the NF and as $\mathbf{J}(\theta)$ changed little in the region of stiffness measurement, we assumed that $\mathbf{J}(\theta)$ was constant. To examine the correlation between the change in stiffness relative to the NF and the corresponding change in joint torque using individual trials, Eq. 9 can be substituted into Eq. 10 and rearranged as:

$$\Delta\mathbf{F} = \left(\mathbf{J}^{-1}\right)^T \begin{bmatrix} d\theta_s\Delta|\tau_s| & d\theta_s\Delta|\tau_e| & d\theta_e\Delta|\tau_e| & 0 \\ 0 & 0 & d\theta_s\Delta|\tau_e| & d\theta_e\Delta|\tau_e| \end{bmatrix} \begin{bmatrix} \alpha_1 \\ \alpha_2 \\ \alpha_3 \\ \alpha_4 \end{bmatrix} \tag{11}$$

where $\mathbf{J}(\theta_{\mathrm{o}})$ is calculated from the joint angles of each subject at the midpoint of the movements θ_{o}. The predicted trajectory was used in combination with the force field equation to calculate the endpoint force applied to the hand by the force field as described above. From the endpoint force and kinematics, the joint torques were then computed using inverse dynamics as explained in the next section. In this way, the difference in joint torque ($\Delta|\tau|$) for force field movements, relative to NF movements could be estimated. On the other side of the equation, the actual difference in force ($\Delta\mathbf{F}$) produced by the perturbation in the force field relative to the NF was calculated directly from the difference in measured restoring force ($d\mathbf{F}$) in the force field and the NF:

$$\Delta\mathbf{F} = \begin{bmatrix} \Delta F_x \\ \Delta F_y \end{bmatrix} = \begin{bmatrix} dF_x^{FF} - dF_x^{NF} \\ dF_y^{FF} - dF_y^{NF} \end{bmatrix} \tag{12}$$

To determine whether the stiffness was being controlled independently of the joint torque necessary to cancel the force exerted by either force field, the parameters α_i in Eq. 11 were determined by linear regression for each subject using the trials in which stiffness was measured. An R^2 value close to 1 would indicate that endpoint stiffness could be explained by the joint torque required to perform the task. An R^2 value close to zero would indicate that overall, from trial to trial, endpoint stiffness was controlled independently of joint torque.

Torque estimation

Time varying muscle torque at the shoulder and elbow was computed using the equations of motion for a two-link planar arm (c.f. Hollerbach and Flash 1982). The joint torque was calculated as:

$$\begin{aligned}\tau_s=&\ddot{\theta}_s(2X\cos\theta_e + Y + Z) + \ddot{\theta}_e(X\cos\theta_e + Y) - \dot{\theta}_e^2 X\sin\theta_e \\ &-2\dot{\theta}_s\dot{\theta}_e X\sin\theta_e - (l_1\sin\theta_s + l_2\sin(\theta_s+\theta_e))F_x \\ &+(l_1\cos\theta_s + l_2\cos(\theta_s+\theta_e))F_y \\ \tau_e=&\ddot{\theta}_e Y + \ddot{\theta}_s(X\cos\theta_e + Y) + \dot{\theta}_s^2 X\sin\theta_e \\ &-l_2\sin(\theta_s+\theta_e)F_x + l_2\cos(\theta_s+\theta_e)F_y \qquad (13)\end{aligned}$$

where:

$$\begin{aligned}X &= m_2 l_1 c_{m2} + m_c l_c c_{mc} \\ Y &= I_2 + m_2 c_{m2}^2 + I_c + m_c c_{md}^2 \\ Z &= I_1 + m_1 c_{m1}^2 + (m_2 + m_c) l_1^2\end{aligned}$$

τ is joint torque, θ is joint angle (defined according to the convention of Mussa-Ivaldi et al. 1985), I is moment of inertia about the center of mass (c_m) of the segment, l is segment length, and m is segment mass. The subscript s refers to the shoulder joint (or the upper arm), e to the elbow (or the lower arm), and c to the wrist cuff. The mass and inertia of the subject's arm segments were estimated from the weight and segment lengths of each subject based on anthropometrical scaling relations (Winter 1990).

EMG measurement of DF adaptation

To examine the muscle activity after learning in the DF, surface EMG was recorded in the NF, after learning in the DF, and during after-effect trials in the DF for four of the six subjects. All EMG was recorded on the same day with the same electrode placement. Activity was recorded from six muscles producing torque at the shoulder and elbow joints. The muscles included two monoarticular shoulder muscles, the pectoralis major and the posterior deltoid, two biarticular muscles, the biceps brachii and the long head of the triceps, and two monoarticular elbow muscles, the brachioradialis and the lateral head of the triceps. The EMG was recorded by using pairs of disposable silver–silver chloride surface electrodes in a bipolar configuration with a separation distance of approximately 2 cm. The skin was thoroughly cleaned with alcohol and prepared by rubbing in electrode paste. Excess paste was wiped from the skin prior to attaching the electrodes. The resistance of each electrode pair was tested to ensure that it was less than 10 kΩ. EMG signals were filtered at 25 Hz (high pass) and 1 kHz (low pass) and sampled at 2 kHz.

EMG during the DF after-effect trials was compared to EMG during NF movements and EMG after complete adaptation to the DF. The rectified EMG was integrated over the entire movement, from 100 ms prior to movement onset until 800 ms after movement onset. Twenty trials were used from each condition and the data for all subjects was used in an ANOVA with subjects as a random variable. A *post hoc* test was then performed on the three conditions using Scheffe's test with a significance level of 0.05. The rectified EMG was smoothed using a 125-point moving average and averaged over 20 trials for the purposes of illustration.

Results

The two force fields investigated in this study produced distinctive perturbations of the trajectories prior to adaptation. Initial trials in the stable VF perturbed the subjects to the left (Fig. 1A), but they quickly learned to compensate for the force field and soon began to make straighter movements. By the fifth trial, subjects usually succeeded in moving to the final target in a single movement. After learning, the trajectories were relatively straight and consistently reached the final target position. Movements in the unstable DF were initially perturbed either to the right or the left (Fig. 1B), depending on the initial deviation in the path. However, again subjects were able to adapt to the force field, successfully completing the task on most trials and exhibiting straight trajectories to the final target. After learning, trajectories in both the

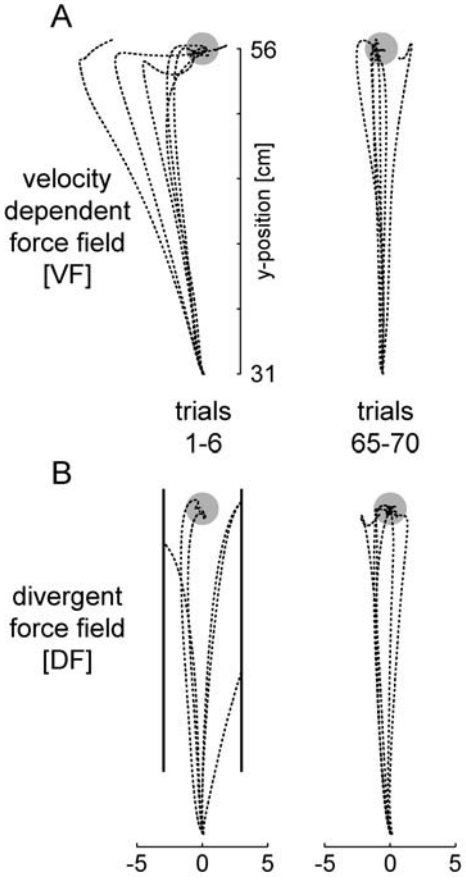

Fig. 1A, B Movements in the force fields, **A** in the velocity-dependent force field (VF) and **B** in the position-dependent (divergent) force field (DF). Movements are shown for the initial movements in the force field (trials 1–6) and the late portion of learning (trials 65–70). The *black lines* on either side of trials 1–6 for the DF indicate the safety zone, outside of which the field was turned off for safety reasons

VF and DF were similar to NF trajectories. The recorded after-effects in the VF were similar to those reported in previous studies using similar force fields (Shadmehr and Mussa-Ivaldi 1994), confirming that subjects adapted to the endpoint forces imposed by the force field. This has been previously suggested to indicate the formation of an internal model of the environmental dynamics (Shadmehr and Mussa-Ivaldi 1994). In the DF, after-effect trajectories deviated less from the straight-line trajectory than did NF movements (Burdet et al. 2001).

Endpoint force after learning

The similarity of trajectories in the VF and the DF to those in the NF indicates that the subjects learned to compensate for the force fields. To compare how compensation for the dynamics was achieved in the two cases, we measured the endpoint force after learning. Figure 2 shows the endpoint force of subject 1 in the NF, VF, and DF averaged over ten movements with standard deviations. Subjects adapted to the VF by counteracting the force produced by the field. The force was more positive in the *x*-direction and more negative in the *y*-direction than in the NF. During the early stages of learning in the DF, subjects experienced large forces which could be either positive or negative depending on the initial movement direction. However, once subjects had adapted to this field, similar endpoint forces were recorded in the DF as had been recorded in the NF.

Figure 3 shows mean endpoint force and standard deviations at the midpoint of the trajectory (time of stiffness measurement) in the three force fields for six subjects. The endpoint force after learning in the VF was significantly larger (positive) in the *x*-direction and significantly smaller (more negative) in the *y*-direction compared to the endpoint force in the NF. For no subject was the *x*- or *y*-force at the midpoint of the movement trajectory in the DF significantly different from that in the NF (Fig. 3). In contrast to the VF, adaptation in the DF did not require a change in the endpoint force.

In order to further examine the difference in adaptation that was required in these two force fields we computed the joint torques using inverse dynamics (Fig. 4). In comparison to the NF, the adaptation to the VF required a larger extensor torque at the shoulder throughout the entire movement and a small extensor torque at the elbow late in the movement to compensate for the force field. Since no change in endpoint force occurred in the DF, the mean joint torque after adaptation was not different from the NF. There was, however, a larger variation in the joint torque in the DF than the NF because force was applied to the hand whenever the trajectory deviated from the *y*-axis. Because this force acted to increase the deviation, variation in the trajectory was also greater in the DF than the NF.

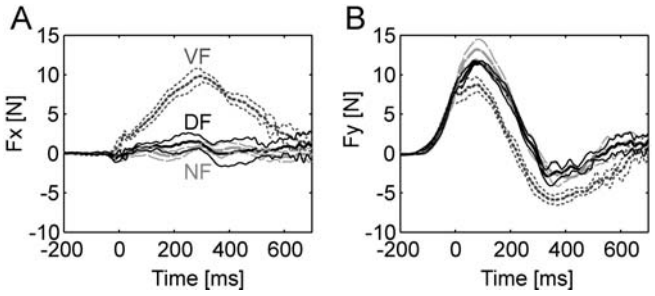

Fig. 2A, B Force profiles after adaptation to the force fields. Mean endpoint force profiles for the *x*- (**A**) and *y*-directions (**B**) during the movement after learning in the null field (NF; *gray*), VF (*dotted*), and DF (*solid black*). Standard deviations are shown for movements based on the last 20 successful trials. Data are shown for one subject

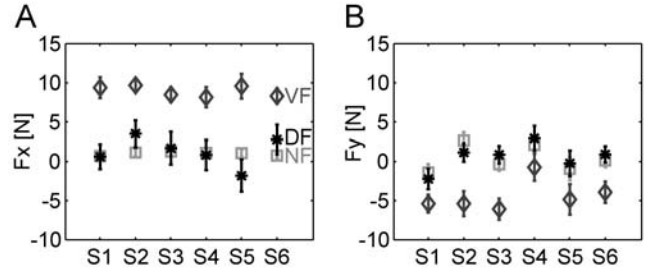

Fig. 3A, B Mean endpoint force after adaptation to the force fields, **A** in the *x*-direction and **B** in the *y*-direction. The mean *x*- and *y*-forces and standard deviations at the midpoint of the movements in the NF (*squares*), VF (*diamonds*), and DF (*stars*) for all six subjects. The time of measurement corresponds to the time at which stiffness was estimated in the movements

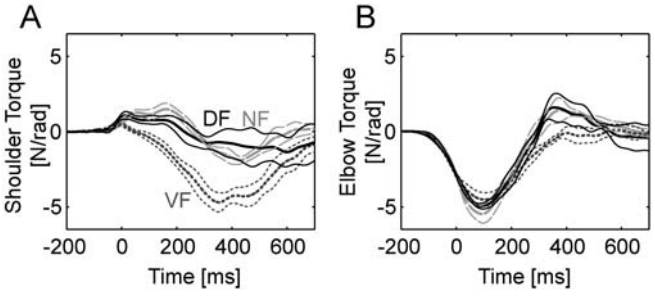

Fig. 4A, B Joint torque profiles after adaptation to the force fields. **A** Shoulder torque. **B** Elbow torque. The shoulder and elbow joint torque profiles are shown for the NF (*gray*), VF (*dotted*), and DF (*solid black*). Adaptation to the VF required an extensor torque at the shoulder whereas no changes in joint torque were observed in the DF. Data are shown for the same subject as Fig. 2

Endpoint stiffness changes with adaptation to force fields

The endpoint stiffness of the arm, measured after adaptation to the NF, VF, and DF is shown in Fig. 5. The ellipses represent stiffness at the midpoint of the movement. In both the VF and DF, the endpoint stiffness was modified in shape and orientation compared to stiffness in the NF. In the VF, the endpoint stiffness

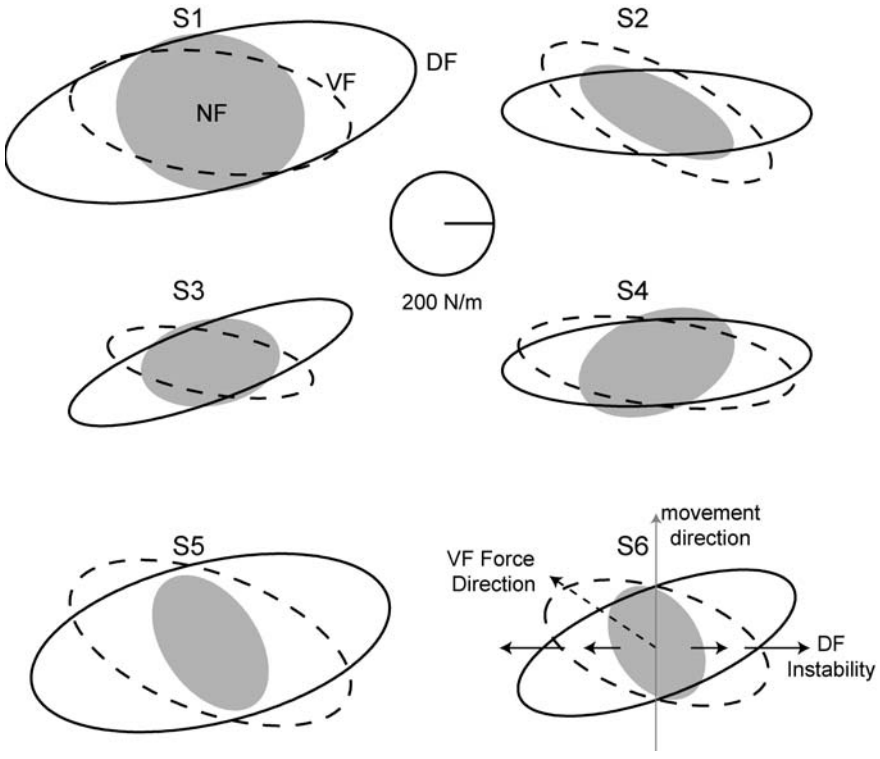

Fig. 5 Stiffness geometry after adaptation to different force fields. Stiffness ellipses are shown for six subjects in the NF (*light gray filled ellipse*), VF (*dotted ellipse*), and DF (*dark solid ellipse*). For the ellipses of subject 6, a *gray arrow* illustrates movement direction and *dotted and solid arrows* show the direction of the external force in the VF and direction of instability in the DF, respectively

increased along the direction of force compensation (Fig. 3), although this occurs only for specific force directions (cf. Gomi and Osu 1998). In the DF the stiffness increased dramatically in the direction of the instability (indicated by *small black arrows* for subject S6), but there was relatively little change in the movement direction. The increase in stiffness in the direction of instability was achieved without a change in the endpoint force (Fig. 3). This illustrates the ability to control the endpoint stiffness of the arm independently of endpoint force as previously described by Burdet et al. (2001).

The endpoint stiffness can be decomposed into two components: a symmetric component (conservative) and an antisymmetric component (rotational) (Mussa-Ivaldi et al. 1985). Neither during estimation nor visualization procedures, did we constrain the endpoint stiffness to be symmetric. For comparison to previous work, the curl components of the endpoint stiffness were estimated as in Mussa-Ivaldi et al. (1985). In particular, we estimated Z_{mean} which is the square root of the ratio of the determinant of the antisymmetric stiffness to the determinant of the symmetric stiffness. Expressed as a percentage, we found the following Z_{mean} values (mean ± SD of six subjects) for stiffness under the three conditions, NF: 23.0±10.8; VF: 15.5±11.1; DF: 24.6±12.9. In general, these are larger than those found under isometric conditions at rest (Mussa-Ivaldi et al. 1985). Differences in Z_{mean} across force fields was tested using an ANOVA with subjects as a random effect. There was no significant difference in the contribution of the antisymmetric component to the endpoint stiffness after adaptation to the DF compared to the NF (P=0.83) or after adaptation to the VF compared to the NF (P=0.28).

Stiffness in VF can be predicted only from change in joint torque

Endpoint stiffness increased in specific directions both for movements in the VF and the DF. However, the reasons for the increase in stiffness were likely different. To address this issue we performed an analysis to determine whether or not stiffness was being controlled independently of the joint torque necessary to compensate for the forces applied by the force field. We used the linear relation represented by Eq. 11 to predict the stiffness and so determine whether the increased stiffness could be explained by increased joint torque relative to NF movements. The change in endpoint force produced by the perturbation used to measure stiffness was estimated for each trial based on the prediction of the unperturbed trajectory and the field strength. Figure 6 compares the measured and estimated changes in endpoint force relative to endpoint force in the NF (ΔF_x and ΔF_y). The parameters α_i were estimated from the data obtained in the VF (left) and DF (right) for each subject using trials where stiffness was measured. From the results it is evident that the stiffness in the VF was relatively well correlated with the applied force, whereas in the DF the correlation was generally poor. The difference in slope for the VF and DF relations demonstrates clearly that stiffness changed for different reasons. For the VF, the slope was close to one indicating that the difference in

joint torque accounts well for the difference in resistive force due to the difference in stiffness relative to the NF. In contrast, for the DF the slope was close to zero for all subjects indicating that the difference in resistive force was independent of the difference in joint torque.

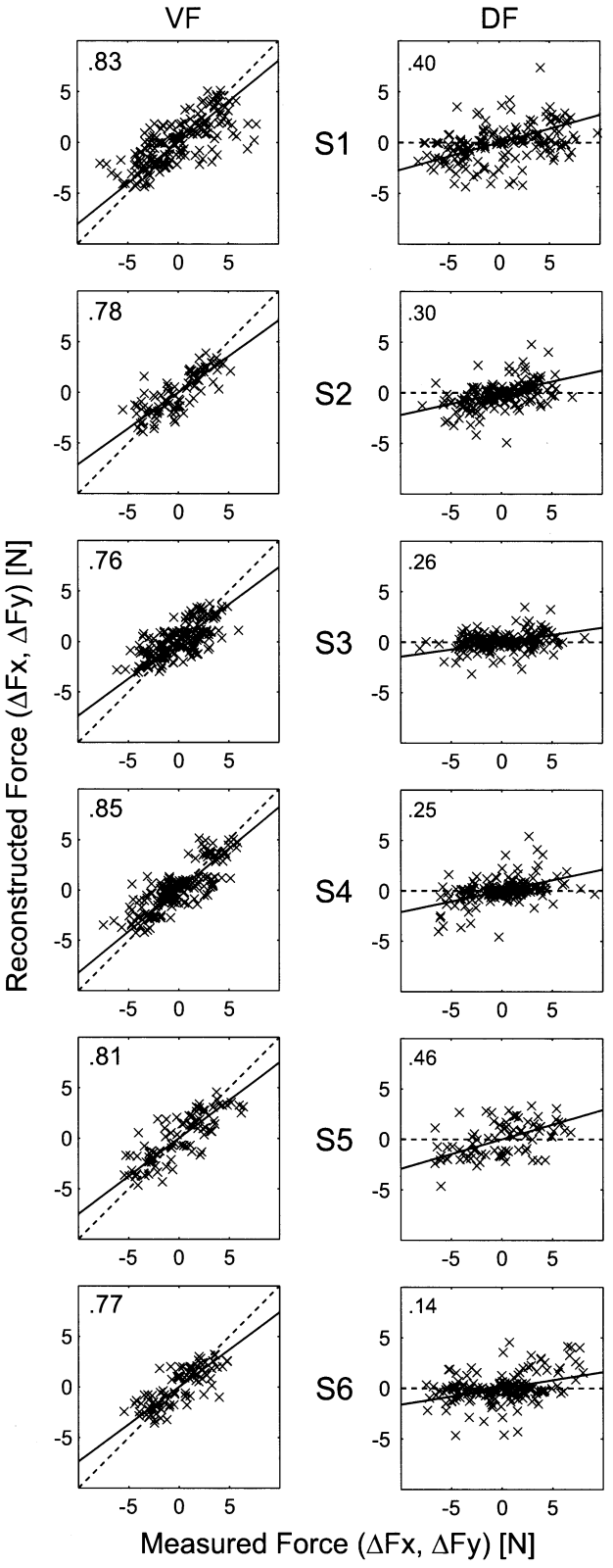

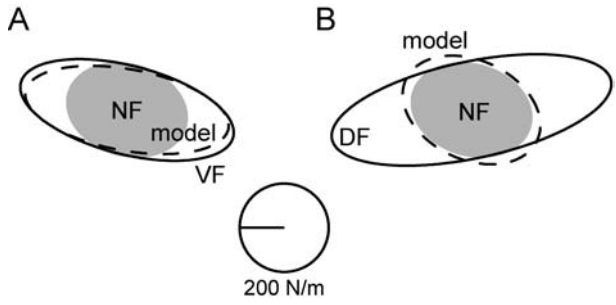

Fig. 7A, B The stiffness geometry predicted by modeling joint stiffness as a linear function of joint torque (Eq. 10; *broken ellipse*) with the stiffness measured in the NF (*gray*) and force field (*solid*) superimposed. **A** VF. **B** DF. Stiffness was computed for individual trials and averaged, using the force data for each subject. The ellipses represent the stiffness averaged across all six subjects

To further investigate how much of the difference in endpoint stiffness could be explained by the difference in joint torque we used Eq. 9 to compute the difference in joint stiffness in the force field relative to the NF, which was then added to the NF stiffness. The parameters α_i were estimated for each subject using the respective data for the VF and DF. The stiffness was computed using force data from individual trials and averaged. The resulting stiffness ellipses in Fig. 7 illustrate the stiffness geometry that would have resulted if the stiffness scaled directly with the calculated joint torques. The modeled stiffness for movements in the VF shows an increase in stiffness along the same direction as the observed stiffness, of almost identical size and shape (Fig. 7A). In the DF, the modeled stiffness is essentially the same as the NF stiffness so the model fails to reproduce the observed increase in stiffness along the direction of instability (Fig. 7B). This indicates that the increased stiffness in the DF was not due to any increase in net joint torque accompanying adaptation to the DF and must, therefore, have been independently modulated due to co-contraction of antagonist muscles or contribution from reflexes.

Joint stiffness changes under VF and DF

The joint stiffness was calculated from the endpoint stiffness matrix (McIntyre et al. 1996). The elements of the joint stiffness matrix in the NF are shown in Fig. 8A.

Fig. 6 Relations between reconstructed and measured changes in force for displacements in the VF (*left*) and DF (*right*). The measured change in force is calculated from the recorded force data during the experiments (Eq. 13). The reconstructed force is based on estimates of the joint torque, the displacement size, and the estimates of α (Eq. 12). Changes of endpoint force in the *x*- and *y*-direction relative to force in the NF (ΔF_x and ΔF_y) are plotted for each subject. R^2 values for the relation, calculated using data from both the *x*- and *y*-directions, are placed in the *top left corner* of each panel. The slope of each relation is shown with the *solid line*. For reference purposes, lines of slope one (VF) and slope zero (DF) are overlaid on each plot with *dotted lines*

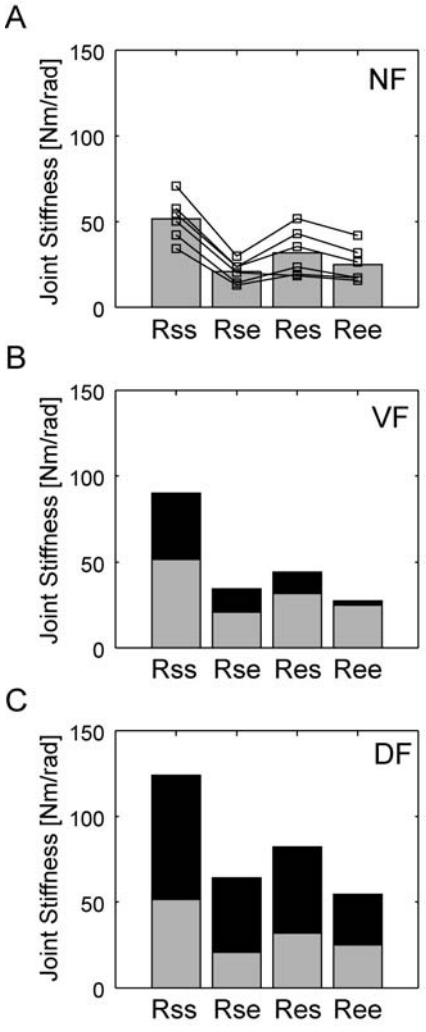

Fig. 8A–C Changes in joint stiffness associated with the change in endpoint stiffness. **A** Joint stiffness in the NF. The *bar graph* shows the mean stiffness for each term in the matrix, whereas the *joined lines* show the individual values for five subjects. **B** Mean joint stiffness after adaptation to the VF (*black bars*) relative to the joint stiffness in the NF (*gray bars*) (same as in **A**). **C** Mean joint stiffness after adaptation to the DF (*black bars*) relative to the joint stiffness in the NF (*gray bars*)

The relative values for all subjects were similar in the NF. After adaptation to the VF, the shoulder joint stiffness (R_{ss}) and cross-joint stiffness (R_{se} and R_{es}) increased by 36.7, 11.7, and 13.8 Nm/rad, respectively, while the elbow joint stiffness (R_{ee}) increased by only 2.9 Nm/rad (Fig. 8B). The greatest changes were in the shoulder joint and cross-joint stiffness terms. This indicates that the major contribution came from the shoulder extensor muscles, followed by the biarticular extensor muscle.

The changes in joint stiffness terms, seen after adaptation to the DF, present a different pattern (Fig. 8C). In this case, the increases in the shoulder joint stiffness term (82.1 Nm/rad) and cross-joint stiffness terms (49.5 and 60.8 Nm/rad) were more comparable, with a somewhat smaller increase in single joint elbow stiffness (39.3 Nm/rad). As the biarticular muscles must contribute to the single joint elbow and shoulder stiffness, as well as to the cross-joint stiffness terms it seems that the single joint muscles likely contribute little to the increased joint stiffness.

One noteworthy point is that in the NF the cross-joint stiffness term, R_{se}, is larger than the elbow stiffness, R_{ee}, for all five subjects. The other cross-joint term, R_{es}, is almost the same as R_{ee}. After adaptation either to the VF or the DF, the cross-joint stiffness terms increased by more than the single joint elbow stiffness term. This finding could be explained by biarticular muscles contributing more to cross-joint stiffness than to single joint elbow stiffness in this condition. The actual contribution to single joint stiffness relative to shoulder stiffness or cross-joint stiffness will be dependent on the ratios of the moment arms of the biarticular muscles at the elbow and shoulder joints.

Stiffness measurements in the DF were performed with the force field turned off prior to the applied perturbation. In order to determine if this could affect the value of the stiffness measurement and to confirm that the stiffness adaptation is preprogrammed, the EMG after adaptation was compared to that during after-effects. Figure 9 compares the EMG during after-effect trials of the DF with that during NF trials. The EMG was much higher during DF trials compared to NF trials ($P<0.001$ for all six muscles), illustrating the large increase in co-contraction in antagonist muscle pairs, and corresponding to the adapted impedance. Similarly, the after-effect EMG was much higher than NF trials ($P<0.001$ for all six muscles) although these movements were also performed in the NF. Furthermore, the EMG during after-effect trials was very similar in magnitude and shape to DF trials. For three muscles there was no significant difference in the magnitude between after-effect and DF trials, posterior deltoid ($P=0.17$), pectoralis major ($P=0.25$), and brachioradialis ($P=0.96$), whereas for the other three muscles the DF EMG was slightly higher than the EMG during after-effects, triceps long head ($P=0.017$), biceps brachii ($P=0.005$), and triceps lateral head ($P=0.022$). Although the DF was off during the after-effect trials, the subjects were not aware on which trials the DF was on or on which it was off, and assumed that it was always on. Thus, the EMG during the after-effect trials reveals a preprogrammed motor command to compensate for the DF. The impedance was predictively and not reactively controlled. Similarly, this indicates that having the force field off prior to the stiffness measurement should not have affected the stiffness measurement. The small differences in EMG between DF and after-effect trials, occurring in the later half of the movement, likely represent the neural feedback response to perturbations caused by the DF. Such perturbations would not have occurred during trials in which stiffness was being measured, regardless of whether the DF had been activated or inactivated prior to the interval of stiffness measurement. Because the differences in EMG were small compared to the overall magnitude of the EMG and because their onset tended to

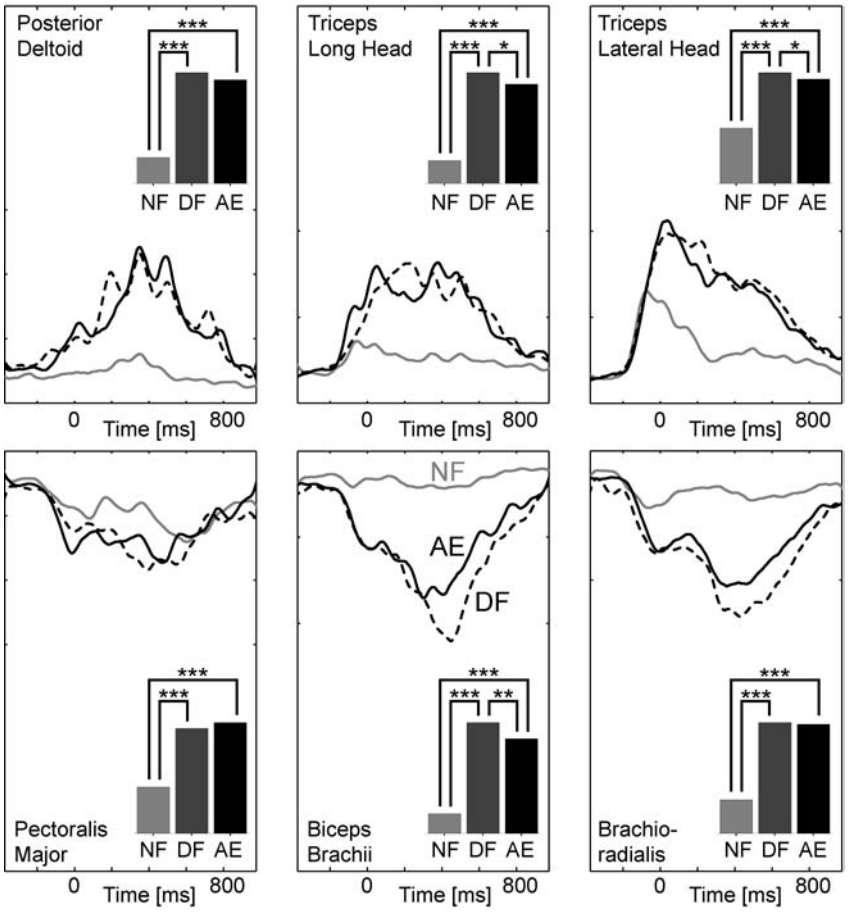

Fig. 9 Rectified, averaged, and smoothed surface EMG during the DF after-effect trials for subject 1. *Black dashed curves* denote EMG in the DF-on trials of the after-effect experiment (DF). *Black solid curves* denote EMG in the NF trials of the after-effect experiment (AE). *Gray curves* denote EMG in NF trials, where the DF was never presented (NF). In each plot the mean integrated EMG activity over the entire movement for all subjects is shown with *bar graphs*. The *asterisks* indicate significant differences between the three conditions using Scheffe's *post hoc* comparison: * $P<0.05$, ** $P<0.01$, *** $P<0.001$

be later than the onset of stiffness measurement, we can be quite certain that the muscles were in the same mechanical state on normal DF trials and on DF trials when stiffness was being measured.

Discussion

This study compared changes in endpoint impedance after adaptation to stable and unstable environments in order to further understand the processes of learning and adaptation. The endpoint stiffness of the arm was modified during adaptation to both environments, but for different reasons. In the stable environment (VF), the change in stiffness was due to changes in the net joint torques needed to counteract the large environmental force. In contrast, the change in stiffness after adaptation to the unstable environment (DF) far exceeded what would have been predicted from the change in joint torques necessary to cancel the environmental force. Furthermore, the change in stiffness was uncorrelated with the change in joint torque. Instead, there was a directionally selective increase in stiffness which was likely brought about by biased co-contraction of biarticular muscles.

Stiffness in stable dynamics is a side effect of change in joint torque

Previous studies which investigated the adaptation of arm movements to novel dynamics did not measure how endpoint stiffness changed after learning, although changes in the EMG of selected muscles were reported (Thoroughman and Shadmehr 1999). While these changes in muscle activity patterns likely corresponded to changes in endpoint stiffness the latter has not been quantified. This is the first quantitative investigation of the change in endpoint stiffness following learning of an internal model.

After adaptation to the VF, the stiffness ellipses became elongated along the direction of compensation for the force field. Such a change in endpoint stiffness with force direction has been reported previously for static postures (Gomi and Osu 1998; McIntyre et al. 1996; Perreault et al. 2001). The observed change in stiffness orientation is similar to that reported by (Gomi and Osu 1998) for the corresponding force direction. We found that the difference in the elastic force, resisting displacement of the hand, relative to the NF was well correlated with the estimated difference in force based on an assumed linear relation between the difference in joint stiffness and the difference in joint torque relative to the NF. Furthermore, the same linear relation generated an excellent prediction of the stiffness measured in the VF.

This is strong evidence that the change in stiffness observed in the VF was simply a byproduct of the change in endpoint force required to adapt to the force field.

Stiffness in unstable dynamics is directly controlled

When subjects were faced with the unstable dynamics of the DF, they responded by selectively adapting their stiffness. This provided necessary stability to perform the task successfully. This impedance control was performed by co-contracting antagonist muscle pairs in order to increase stiffness without changing the net joint torque. Such impedance control was first postulated by Hogan (1985). While EMG measurements during movements to a single point from various starting positions provided some limited evidence that impedance may vary depending on past history (Gribble and Ostry 1998), no conclusive evidence for the existence of impedance control had been found until recently (Burdet et al. 2001).

While reflexes could have contributed to the measured stiffness it is unlikely that they were responsible for the adaptation which permitted stable movement in the DF. Reflexes would only act following displacement of the hand from the planned trajectory and would occur too late to counteract the DF because its effect would be increasing throughout the delay period. Since the trajectories in the DF after learning were similar to those in the NF, with the hand moving smoothly to the final target, there is no evidence that the hand was sufficiently disturbed to evoke reflex responses.

Because measurements of stiffness are based on multiple trials they contain no information about trial-by-trial variations. Although unlikely, it is possible that the observed increase in stiffness was linked to the force which the subject exerted to counteract the force applied by the force field. This would vary from trial to trial due to variations in the trajectory. If this had been the case, then the difference in stiffness, relative to the NF, should have given a change in force which was correlated with the difference in measured endpoint force. When this was tested we found that the two were essentially independent. Similarly, stiffness ellipses generated from presumed linear relations between joint torque and joint stiffness failed to reproduce the measured endpoint stiffness in the DF. From this, it is clear that the change in endpoint stiffness in the DF with respect to the NF could not be attributed to compensation for the small forces exerted by the force field. Therefore, we can conclude that after adaptation to the unstable DF, the stiffness was controlled independently of the endpoint force and was selectively tuned to the instability of the environment.

Change in stiffness is a byproduct of development of an inverse model

As the CNS learns to adapt to the environment, the activity of the muscles is modified in order to counteract the environmental dynamics. This is presumed to occur during formation of an inverse model of the dynamics (Conditt et al. 1997; Flanagan and Wing 1997; Flanagan et al. 2001; Krakauer et al. 1999; Shadmehr and Mussa-Ivaldi 1994; Thoroughman and Shadmehr 1999). Because muscle stiffness increases linearly with muscle activation and force (Hunter and Kearney 1982; Kirsch et al. 1994), any change in the activation produced by the development of an internal model should produce a corresponding change in stiffness. We found that the change in limb impedance was well explained by the change in the joint torque that occurred during the learning in the VF. The only other study which has attempted to address changes in the impedance of the arm after adaptation to novel force fields is the recent work of Wang et al. (2001). They proposed that an inverse model would not have any effect on the impedance of a limb and specifically would not change the intrinsic stiffness or the short latency reflex response to a perturbation. The restoring force due to large perturbations during movements was attributed to the long latency reflex and it was presumed that the gain of this reflex was changed due to a modification of the sensory-motor feedback control pathway (Wang et al. 2001). This conclusion is based upon the assumption that the use of an inverse model to adapt to the environment would not affect the intrinsic or reflexive stiffness of a muscle. However, modifying the feedforward command to muscles will automatically change both the intrinsic and reflexive components of the muscle impedance. As the descending drive to muscles (activation) is increased the muscle's force response to a disturbance (impedance) increases. This has been shown at both the muscle level (Kirsch et al. 1994) and joint level (Carter et al. 1990, 1993; Gottlieb and Agarwal 1988; Hunter and Kearney 1982; Milner et al. 1995; Weiss et al. 1988). Similarly, previous work has also shown that both the short and long latency reflexes are directly influenced by the level of muscle activation (Capaday et al. 1994; Dufresne et al. 1978; Marsden et al. 1976; Matthews 1986; Smeets and Erkelens 1991; Stein et al. 1995). These results indicate that any change in the activation level of a muscle due to a modification in the descending command, such as would be produced by an inverse model would affect both the intrinsic and reflexive stiffness of the muscles. This is also seen in the multijoint arm where a change in the joint torque has a direct effect on the joint stiffness and, therefore, the endpoint stiffness (Gomi and Osu 1998; Perreault et al. 2001). A key issue is the question of whether the change in impedance following adaptation to novel dynamics is due to a change in intrinsic and reflexive stiffness which occurs as a direct effect of a change in motor command, or if it is due to the modification of the sensory-motor feedback pathway. The results of our analysis on adaptation to the VF clearly indicate that the change in impedance scales with the change in joint torque, exactly as in isometric multijoint tasks (Gomi and Osu 1998; Perreault et al. 2001) where no change to the sensory-motor feedback pathways is required. This indicates that development of an inverse

model can directly affect the limb impedance. This must be taken into account when using the force responses to perturbations to infer the properties of the motor control system.

Acknowledgements The experiments were performed at ATR. We thank T. Yoshioka for his technical assistance. The manipulandum was setup by T. Yoshioka and H. Gomi. This research was supported by the Telecommunications Advancement Organization of Japan, the Natural Sciences and Engineering Research Council of Canada, the Swiss National Science Foundation, and the Human Frontier Science Program

References

Akazawa K, Milner TE, Stein RB (1983) Modulation of reflex EMG and stiffness in response to stretch of human finger muscle. J Neurophysiol 49:16–27

Bennett DJ (1993) Torques generated at the human elbow joint in response to constant position errors imposed during voluntary movements. Exp Brain Res 95:488–498

Buchanan TS, Almdale DPJ, Lewis JL, Rymer WZ (1986) Characteristics of synergic relations during isometric contractions of human elbow muscles. J Neurophysiol 56:1225–1241

Burdet E, Osu R, Franklin DW, Yoshioka T, Milner TE, Kawato M (2000) A method for measuring endpoint stiffness during multijoint arm movements. J Biomech 33:1705–1709

Burdet E, Osu R, Franklin DW, Milner TE, Kawato M (2001) The central nervous system stabilizes unstable dynamics by learning optimal impedance. Nature 414:446–449

Cannon SC, Zahalak GI (1982) The mechanical behavior of active human skeletal muscle in small oscillations. J Biomech 15:111–121

Capaday C, Forget R, Milner T (1994) A re-examination of the effects of instruction on the long-latency stretch reflex response of the flexor pollicis longus muscle. Exp Brain Res 100:515–521

Carter RR, Crago PE, Keith MW (1990) Stiffness regulation by reflex action in the normal human hand. J Neurophysiol 64:105–118

Carter RR, Crago PE, Gorman PH (1993) Nonlinear stretch reflex interaction during cocontraction. J Neurophysiol 69:943–952

Conditt MA, Gandolfo F, Mussa-Ivaldi FA (1997) The motor system does not learn the dynamics of the arm by rote memorization of past experience. J Neurophysiol 78:554–560

Dufresne JR, Soechting JF, Terzuolo CA (1978) Electromyographic response to pseudo-random torque disturbances of human forearm position. Neuroscience 3:1213–1226

Flanagan JR, Wing AM (1997) The role of internal models in motion planning and control: evidence from grip force adjustments during movements of hand-held loads. J Neurosci 17:1519–1528

Flanagan JR, King S, Wolpert DM, Johansson RS (2001) Sensorimotor prediction and memory in object manipulation. Can J Exp Psychol 55:87–95

Flanders M, Soechting JF (1990) Arm muscle activation for static forces in three-dimensional space. J Neurophysiol 64:1818–1837

Gomi H, Kawato M (1996) Equilibrium-point control hypothesis examined by measured arm stiffness during multijoint movement. Science 272:117–120

Gomi H, Kawato M (1997) Human arm stiffness and equilibrium-point trajectory during multi-joint movement. Biol Cybern 76:163–171

Gomi H, Osu R (1998) Task-dependent viscoelasticity of human multijoint arm and its spatial characteristics for interaction with environments. J Neurosci 18:8965–8978

Gottlieb GL, Agarwal GC (1988) Compliance of single joints: elastic and plastic characteristics. J Neurophysiol 59:937–951

Gribble PL, Ostry DJ (1998) Independent coactivation of shoulder and elbow muscles. Exp Brain Res 123:355–360

Groeningen CJ van, Erkelens CJ (1994) Task-dependent differences between mono- and bi-articular heads of the triceps brachii muscle. Exp Brain Res 100:345–352

Hogan N (1985) The mechanics of multi-joint posture and movement control. Biol Cybern 52:315–331

Hollerbach MJ, Flash T (1982) Dynamic interactions between limb segments during planar arm movement. Biol Cybern 44:67–77

Hunter IW, Kearney RE (1982) Dynamics of human ankle stiffness: variation with mean ankle torque. J Biomech 15:747–752

Karst GM, Hasan Z (1991) Timing and magnitude of electromyographic activity for two-joint arm movements in different directions. J Neurophysiol 66:1594–1604

Kirsch RF, Boskov D, Rymer WZ (1994) Muscle stiffness during transient and continuous movements of cat muscle: perturbation characteristics and physiological relevance. IEEE Trans Biomed Eng 41:758–770

Krakauer JW, Ghilardi MF, Ghez C (1999) Independent learning of internal models for kinematic and dynamic control of reaching. Nat Neurosci 2:1026–1031

Lacquaniti F, Carrozzo M, Borghese NA (1993) Time-varying mechanical behavior of multijointed arm in man. J Neurophysiol 69:1443–1464

Marsden CD, Merton PA, Morton HB (1976) Stretch reflex and servo action in a variety of human muscles. J Physiol 259:531–560

Matthews PB (1986) Observations on the automatic compensation of reflex gain on varying the pre-existing level of motor discharge in man. J Physiol 374:73–90

McIntyre J, Mussa-Ivaldi FA, Bizzi E (1996) The control of stable postures in the multijoint arm. Exp Brain Res 110:248–264

Milner TE, Cloutier C, Leger AB, Franklin DW (1995) Inability to activate muscles maximally during cocontraction and the effect on joint stiffness. Exp Brain Res 107:293–305

Mussa-Ivaldi FA, Hogan N, Bizzi E (1985) Neural, mechanical, and geometric factors subserving arm posture in humans. J Neurosci 5:2732–2743

Osu R, Gomi H (1999) Multijoint muscle regulation mechanisms examined by measured human arm stiffness and EMG signals. J Neurophysiol 81:1458–1468

Perreault EJ, Kirsch RF, Crago PE (2001) Effects of voluntary force generation on the elastic components of endpoint stiffness. Exp Brain Res 141:312–323

Rancourt D, Hogan N (2001) Stability in force-production tasks. J Mot Behav 33:193–204

Schmidt RA, Zelaznik H, Hawkins B, Frank JS, Quinn JT Jr (1979) Motor-output variability: a theory for the accuracy of rapid motor acts. Psychol Rev 47:415–451

Shadmehr R, Mussa-Ivaldi FA (1994) Adaptive representation of dynamics during learning of a motor task. J Neurosci 14:3208–3224

Slifkin AB, Newell KM (1999) Noise, information transmission, and force variability. J Exp Psychol Hum Percept Perform 25:837–851

Smeets JB, Erkelens CJ (1991) Dependence of autogenic and heterogenic stretch reflexes on pre-load activity in the human arm. J Physiol 440:455–465

Stein RB, Hunter IW, Lafontaine SR, Jones LA (1995) Analysis of short-latency reflexes in human elbow flexor muscles. J Neurophysiol 73:1900–1911

Tax AA, Denier van der Gon JJ, Gielen CC, Tempel CM van den (1989) Differences in the activation of m. biceps brachii in the control of slow isotonic movements and isometric contractions. Exp Brain Res 76:55–63

Tax AA, Denier van der Gon JJ, Erkelens CJ (1990a) Differences in coordination of elbow flexor muscles in force tasks and in movement tasks. Exp Brain Res 81:567–572

Tax AA, Denier van der Gon JJ, Gielen CC, Kleyne M (1990b) Differences in central control of m. biceps brachii in movement tasks and force tasks. Exp Brain Res 79:138–142

Thoroughman KA, Shadmehr R (1999) Electromyographic correlates of learning an internal model of reaching movements. J Neurosci 19:8573–8588

Wadman WJ, Denier van der Gon JJ, Derksen RJA (1980) Muscle activation patterns for fast goal-directed arm movements. J Hum Mov Stud 6:19–37

Wang T, Dordevic GS, Shadmehr R (2001) Learning the dynamics of reaching movements results in the modification of arm impedance and long-latency perturbation responses. Biol Cybern 85:437–448

Weiss PL, Hunter IW, Kearney RE (1988) Human ankle joint stiffness over the full range of muscle activation levels. J Biomech 21:539–544

Winter DA (1990) Biomechanics and motor control of human movement. Wiley, New York